

# Innovative cryogenic processing for enhanced surface integrity characteristics of stainless steels

KITAY Ozhan<sup>1,a\*</sup> and KAYNAK Yusuf<sup>2,b</sup>

<sup>1</sup> Department of Machine and Metal Technologies, Bilecik Seyh Edebali University, 11100 Bilecik, Türkiye

<sup>2</sup> Department of Mechanical Engineering, Marmara University, 34854, Istanbul, Türkiye

<sup>a</sup>ozhan.kitay@bilecik.edu.tr, <sup>b</sup>yusuf.kaynak@marmara.edu.tr

**Keywords:** Liquid Nitrogen (LN<sub>2</sub>), Cryogenic, Stainless Steel, Surface Integrity, Machining

**Abstract.** In this study, the influence of the orthogonal cutting on the surface integrity characteristics of 316L austenitic stainless steel material under liquid nitrogen (LN<sub>2</sub>) condition was investigated. For this purpose, machining tests were carried out by applying LN<sub>2</sub> to the cutting tool rake and flank face separately, and using different cutting parameters. In addition to the cutting force, the response of surface integrity characteristics such as microstructure, microhardness, and x-ray diffraction (XRD) analysis to LN<sub>2</sub> was compared with dry cutting. The findings showed that the effect of different positioning of the LN<sub>2</sub> nozzle on the cutting force and microhardness of the material is significant. In particular, the application of liquid nitrogen through the rake face significantly increases the microhardness of the material, while machined specimen microstructure images show that application of LN<sub>2</sub> from the flank surface causes more grain refinement and deformation on the machined surface, especially at low cutting speed.

## Introduction

The 316L austenitic stainless steel has a wide range of uses in biomedical implant manufacturing due to its biocompatibility and is also used in the automotive industry [1-3]. Stainless steel materials are widely used in many industries due to their high strength, toughness, mechanical properties at high temperatures and corrosion resistance [4]. They are called hard-to-cut materials because these characteristic features create difficulties in machining operations [5]. The high cutting forces and cutting temperature during machining of these materials affect the tool wear and the chip breakability. The surface quality, fatigue life and corrosion resistance of the finished product are also affected by these problems [6, 7].

Numerous lubricants and coolants are used to improve the machining performance of the materials in the hard-to-cut materials group [8-10]. In comparison with other cooling and lubrication methods, cryogenic cooling method is an effective method for human and environmental health, besides liquid nitrogen (LN<sub>2</sub>) is widely used as cryogenic coolant in the machining process [11, 12]. In the machining process, cryogenic coolant can be applied to the tool-chip interface or directly to the workpiece. Thus, it penetrates the cutting zone between the tool and chip and reduces the friction coefficient [13-15]. Cryogenic machining is also preferred because it positively affects the surface integrity characteristics of the machined part, such as surface and subsurface hardness change, microstructure, phase transformation, residual stress and fatigue life, which directly affect product performance [15-17].

There are studies in the literature in which cryogenic coolants are applied to increase the functional performance of difficult-to-cut materials in terms of fatigue life, corrosion resistance and wear, and their effects on surface hardness, phase transformation and residual stress formation are also examined [9, 14, 17-19]. Although there are studies examining the changes in the surface

integrity characteristics of cryogenic machining of many different materials in the group of hard-to-cut materials, studies on the surface integrity characteristics of the cryogenic machining of 316L stainless steel have been limited in particular [20].

In this study, the effects of applying LN<sub>2</sub> to cutting area in the 316L stainless steel machining process from rake and flank face at different cutting parameters on the surface integrity characteristics were determined and compared with dry condition in terms of microhardness, microstructure and X-ray diffraction(XRD) analysis.

**Experimental Setup**

The workpieces used in this study were 316L austenitic stainless steel as discs of 50 mm diameter and 3 mm thickness for orthogonal cutting. Hardness of workpiece is 190±5 HV at room temperature. Discs were machined from 50 mm to 33 mm diameter in orthogonal cutting. The chemical composition and mechanical properties of workmaterial are shown in Table 1 and Table 2, respectively.

*Table 1. Chemical composition of 316L austenitic stainless steel [21]*

ELEMENT	C	M	Si	S	P	Cr	Ni	Mo	N	Fe
%	0.02	1.77	0.46	0.027	0.029	16.76	10.09	2.02	0.06	Bal.

*Table 2. Mechanical Properties of 316L austenitic stainless steel [21]*

Yield Stress	Compression Stress	Elongation	Elasticity Module
319 MPa	628 MPa	55 %	200 GPa

The machining experiments were conducted on a Doosan CNC turning center which has maximum spindle speed of 4500 rpm and 18 kW power. In machining operations, TCMW16T308 HTI10 with -2° rake angle, 7° clearance angle and 23 μm edge radius uncoated carbide cutting tool was used. Cutting speeds were selected as 40, 120 and 200 m/min and uncut chip thicknesses (*t<sub>o</sub>*) were 0.08, 0.12 and 0.16 mm. Machining operations were performed under dry machining without any coolant/lubricant, and cryogenic cooling with LN<sub>2</sub> (15 bar) from rake face and flank face conditions. Implementation of cryogenic machining is shown in Fig. 1. All experiments were performed twice for reproducibility. Cutting forces were measured with KISTLER 2129AA dynamometer.

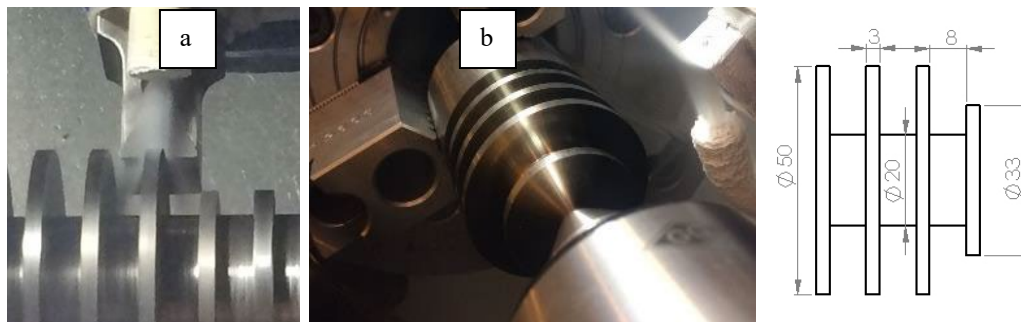


*Fig. 1. Applying LN<sub>2</sub> in orthogonal machining a) from rake face b) from flank face*

To examine the surface integrity characteristics (microhardness, microstructure, phase transformation), machined workpieces were cut with diamond cutting disk then cut specimens were cold-mounted in acrylic and then polished using 60, 30 and 15 μm grit magnetic discs. Specimens were etched using a solution of 2 ml HNO<sub>3</sub> + 4 ml Glycerine + 6 ml HCl to review the microstructure [22]. Microstructure of etched specimens were examined by Olympus BX51M Optic Microscopy. Microhardness of workpiece was measured by using Future-Tech FM310e.

Each hardness of specimen was determined by average of four measurement after applying 25 gf during 15 second to machined specimens. X-ray diffraction (XRD) was used by Bruker AXS D2 Phaser XRD device. CuK $\alpha$  cathode with wavelength of 1.54060 Å, current of 10 mA and voltage of 30 kV were used to analysis the XRD patterns of machined specimens.

### Experimental Results and Discussion

**Cutting Forces.** Cutting forces is an useful indicator to evaluation the machining performance and explain the reasons for the origin of the machining. Cutting forces measured in orthogonal machining process under different cutting conditions is shown in Fig. 2 as a function of cutting speed. A significant reduction in cutting forces is seen with increased cutting speed. The reduction in cutting forces is not only seen in dry cutting, but also in all cutting conditions. Liquid LN<sub>2</sub> evaporates in the cutting area and reduces friction by creating an LN<sub>2</sub> cushion between the tool and the chip. This reduces the strength of the welded junctions between the tool and the chip, allowing less force to be consumed compared to dry cutting. Increasing the cutting speed increases the deformation rate of the workpiece material, resulting in thermal softening of the material and ultimately reduction of the cutting forces. Measured cutting forces when cryogenic coolant applied from rake face is lower than cryogenic applied from flank face. The low cutting forces at the rake face condition can be explained by the effective penetration of the cryogenic coolant at the tool-chip interface and the reduction of friction. This is supported by the fact that the percentage differences are especially high at low cutting speeds. There is a difference of 30% at a cutting speed of 40 m/min. There is also a difference of 12% between the lowest and highest cutting force values at a cutting speed of 120 m/min. Therefore, mechanical effect plays a dominant role at low cutting speeds and when the friction is higher, application of liquid nitrogen through the rake face has shown lubrication effect and reduced forces. By applying liquid nitrogen from the flank face, reductions in cutting forces occurred similar to the rake face. In fact, the workpiece is cooled and this increases its resistance to plastic deformation compared to rake face.

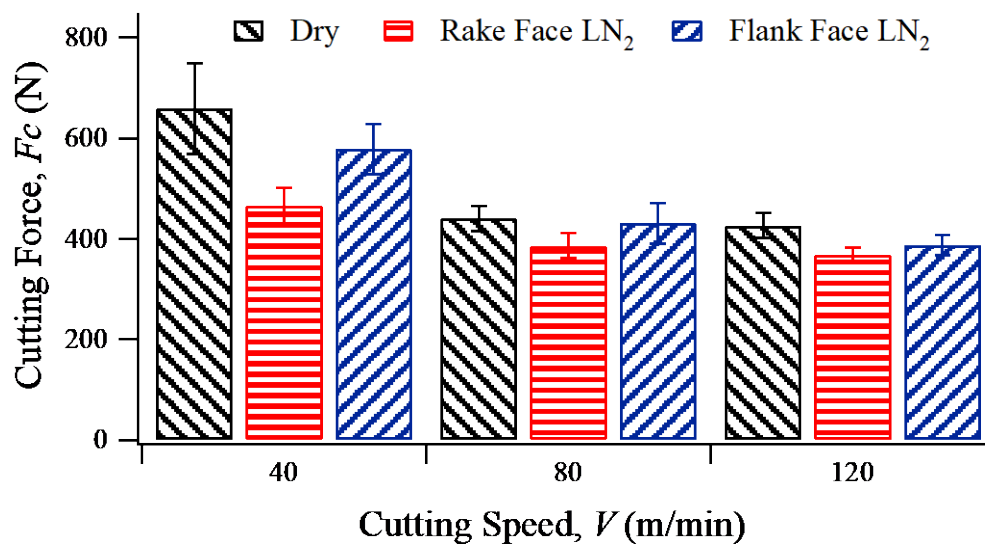


Fig. 2. Measured cutting forces in orthogonal turning as a function of cutting speed ( $t_o = 0.08$  mm)

Cutting forces measured in orthogonal machining process under different cutting conditions is shown in Fig. 3 as a function of cutting depth. While the highest cutting forces were measured in dry cutting, the lowest cutting forces were obtained by applying liquid nitrogen to the rake face. The fact that increasing cutting depth does not negatively affect the penetration ability of liquid nitrogen can be considered as an additional finding. It is expected that the increase in cutting depth causes an increase in cutting forces due to the increase in chip cross-section. Taking dry cutting as

a reference at a cutting depth of 0.16 mm, the decrease in cutting force caused by the application of liquid nitrogen from the rake surface is approximately 20%. However, this ratio is less at the lowest cutting depth. Therefore, it is seen that the lubricating effect of liquid nitrogen plays an active role here as well and can reduce the force more when the friction force is greater.

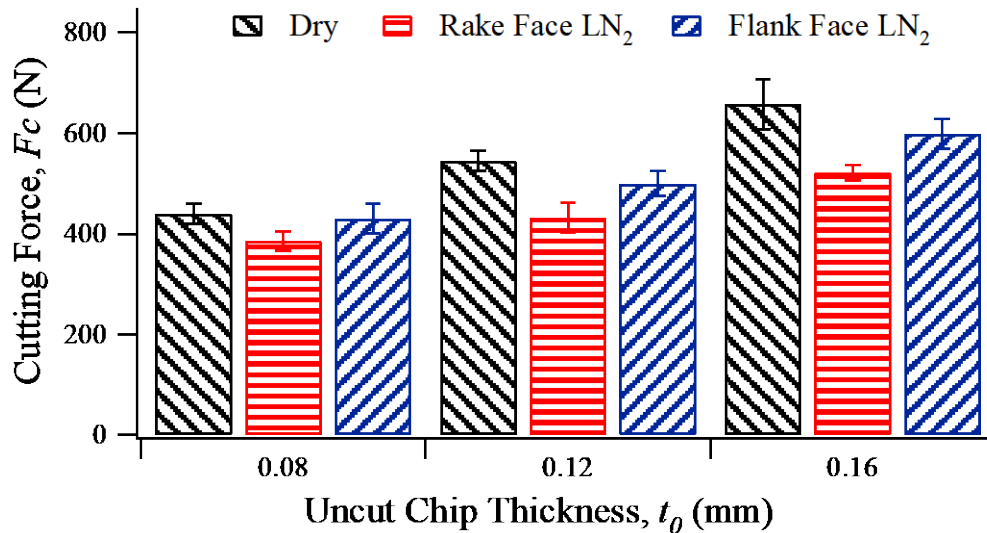


Fig. 3. Effect of cutting depth on cutting forces ( $V=120$  m/min ).

Microhardness. The variation of hardness in the surface and subsurface areas of the machined parts is important depending on where the part will be used. While in some cases it is not desired to change the hardness in order to create a more homogeneous structure, in some cases it is a desirable feature to increase the hardness of the surface, especially in parts that are in contact with each other or subject to wear [23, 24]. 316L has a lower workability than other stainless steels and has a high tendency to hardening during machining [3]. Thermal effects during machining and martensite formation in the austenite structure during plastic deformation are considered as the reason for the tendency of hardening [25, 26].

Microhardness values of orthogonally machined samples under different cutting conditions is shown in Fig. 4. There is an increase in the hardness of the machined samples from surface and sub-surface to 100  $\mu$ m depth in all of conditions. While the highest hardness value was measured as 282 HV under cryogenic condition applied from rake face, the lowest hardness value was measured as 231.5 HV under dry condition at the distance of 15  $\mu$ m from the surface. There is a difference of 22% between the lowest and the highest hardness values. Also, there are increase of 44% and 18% in hardness of machined samples as compared to as-received hardness. LN<sub>2</sub> directly penetrates the tool-chip region from rake face. Therefore, since the primary and secondary deformation region temperature is directly affected, chip breakability becomes easier, but the material hardness increases. However, when LN<sub>2</sub> penetrates from the flank face, the hardness increase is less as the clearance zone is affected.

In Fig. 5, the variation of the hardness from the machined surface to the center of the workpiece can be expressed in three steps. The first stage is hardened very clearly but hardness values is lower than beginning of the second stage. The reason for this behavior is that the first 10  $\mu$ m layer, which is the closest layer to the surface, is the most exposed to heat and high plastic deformation. This has naturally caused a relative decrease in hardness. At the starting point of the second stage, the hardness value reached its maximum point. While the material is exposed to a large plastic deformation, it is exposed to less heat. The depth of this layer determines the surface and the deformed layer under the surface in the result of the machining process. In the third stage, the as-received material hardness is active and the effect of the machining process is not exist.

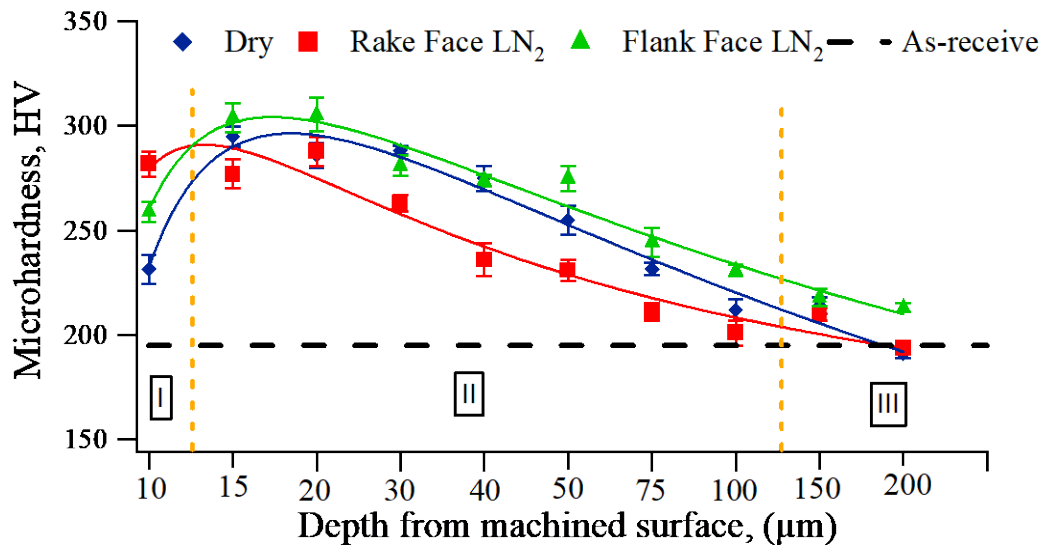


Fig. 4. Microhardness values at different cutting conditions in orthogonal cutting ( $V=120$  m/min,  $t_o= 0.08$  mm)

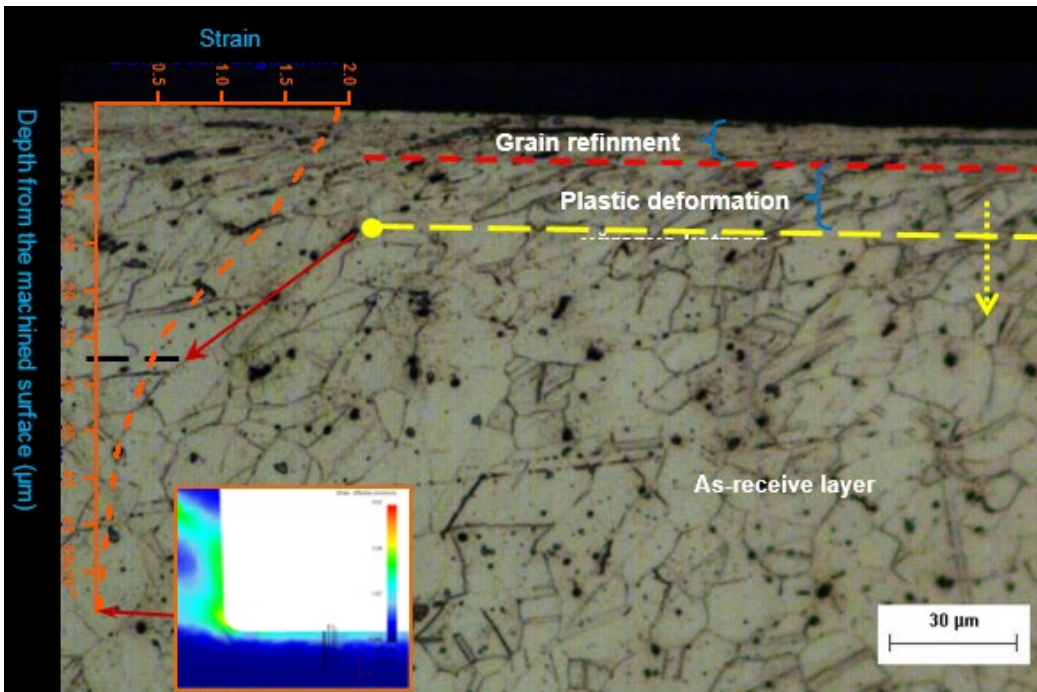


Fig. 5. Plastic deformation behavior of 316L stainless steel material ( $V= 40$  m/dak,  $t_o= 0.08$  mm)

Microhardness values from surface to depth of 200  $\mu\text{m}$  of orthogonally machined samples under different cutting conditions is shown in Fig. 6. There is an increase in all of cutting conditions. It is obvious that hardness values in cryogenic conditions is higher than dry condition. This is an indication that the thermal effect in the surface region will be relatively reduced by the effect of cryogenic cooling. There are increase of 70%, 48% and 37% in hardness of machined samples under LN<sub>2</sub> from rake face, LN<sub>2</sub> from flank face and dry cutting conditions, respectively, as compared to as-received hardness.



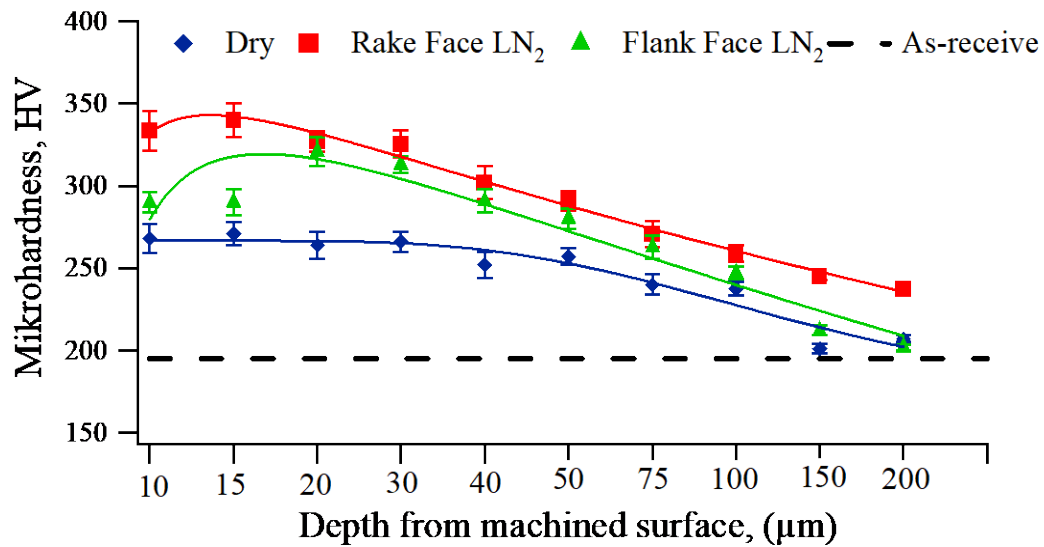
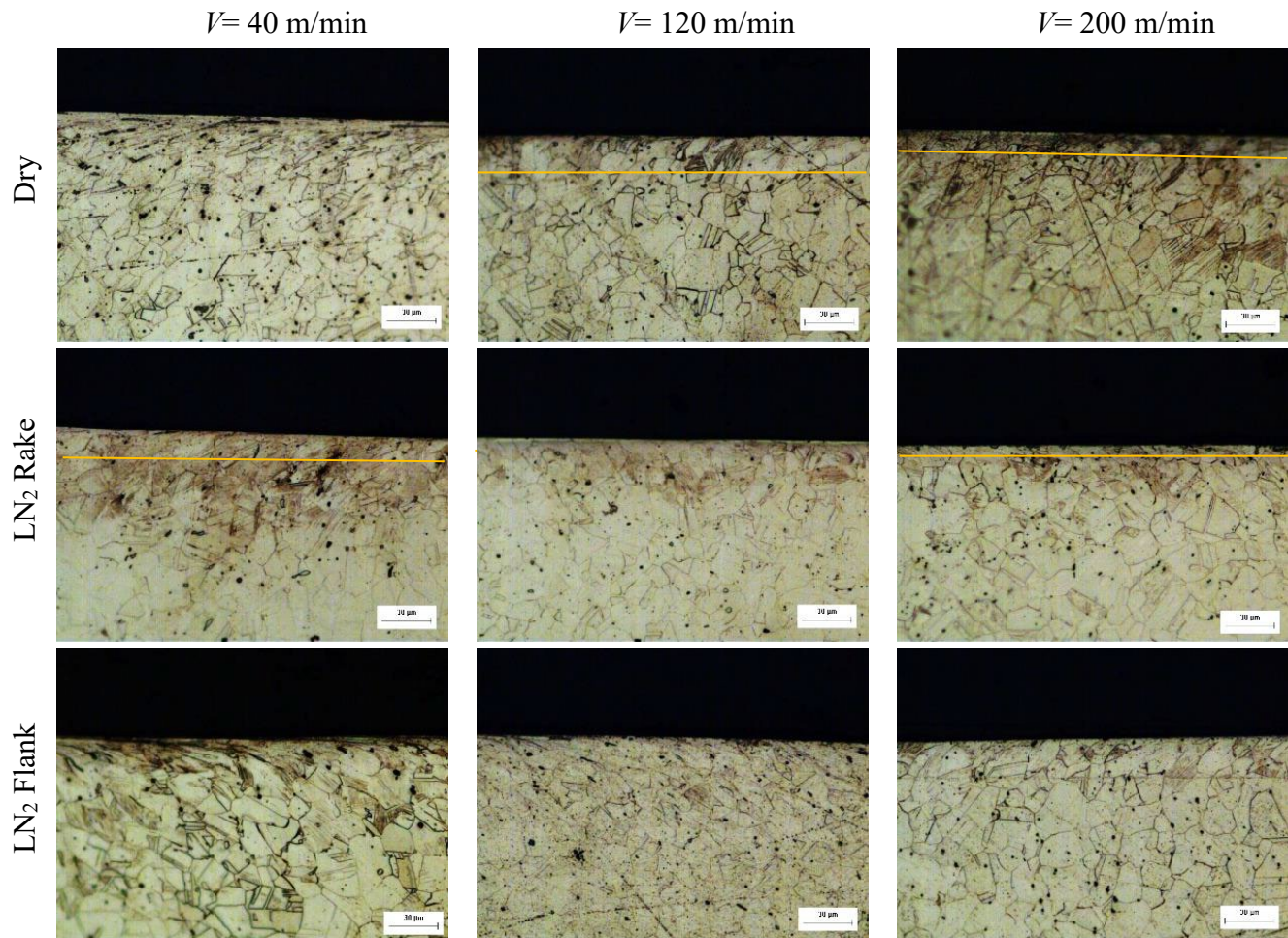


Fig. 6. Microhardness values at different cutting conditions in orthogonal cutting ( $V=120$  m/min,  $t_o=0.16$  mm)

Microstructure Analysis. It is important to examine the microstructure to understand the changes that occur on the workpiece surface and sub-surface after machining. In machining operations, significant changes can be observed in the surface and sub-surface microstructure in terms of cutting conditions and cutting parameters [23, 24, 27]. Since these changes may affect the functionality of the workpiece, the effects of changes occurring in the surface and subsurface areas as a result of machining the workpiece must be determined [15].

Microstructural images of orthogonally machined 316L stainless steel material at different cutting speeds and cutting conditions are shown in Fig. 7. The deformation at the lower cutting speeds at the surface and sub-surface is more obvious than the higher cutting speeds. It is seen that increasing the cutting speed tends to decrease the depth of grain deformation. This can be assessed as an increase in cutting temperature, depending on the increase in cutting speed, and a reflection on the machined surface and sub-surface. It is known that in the machining of different materials, deformation occurs depending on the cutting speed and thus phase transformation occurs in the material. As the cutting speed increases, the cutting temperature increases and the deformation decreases due to the annihilation of dislocations on the machined surface [28].

Also, when cryogenic conditions are compared to dry cutting, it appears that there are no significant differences in terms of microstructure. However, it should be emphasized that cryogenic conditions can be said that they have affected layers at a lower depth than dry cutting, especially considering cutting speeds of 120 and 200 m/min. In general, the temperature of the workpiece during dry cutting is higher than in cryogenic conditions. In this case, even under relatively low stresses, the formation of dislocations can be more convenient and the deformed layers of the workpieces can be larger.



*Fig. 7. Microstructure images of orthogonally turned samples at different cutting speeds and conditions under optical microscope ( $t_o = 0.08$  mm)*

**X-Ray Diffraction Analysis.** In the machining process, changes occur in the surface and subsurface regions of the workpiece depending on the amount of deformation in the cutting area due to effects such as temperature increase, friction and wear, and phase transformation may occur depending on the processing parameters and conditions [15, 23, 24]. Taking into account the austenitic stainless steels, plastic deformation at low temperatures causes austenite-martensite transformation in the structure [29]. This transformation directly affects functional performance criteria such as yield stress, hardening, fracture toughness and fatigue life [30]. The phase transformation caused by the machining process in this context is considered as one of the important surface integrity characteristics [15].

316L stainless steel is a  $\gamma$ -austenitic material with face-centered cubic crystal structure [26]. In 316L stainless steels, martensite phases can be seen or martensite formation can be seen under the effect of tension called SIM (stress induced martensite). This is also a condition that depends on the cutting conditions, which is an unusual situation in the machining process [20, 26]. There are studies stating that cryogenic conditions cause martensite phase formation, but this is only possible with maximum plastic deformation at very low cutting speeds [20, 31, 32].

Fig. 8 shows the comparisons of the main austenite XRD pattern with (111) texture of orthogonally machined samples under different cutting conditions at 120 m/min cutting speed. Looking at the figure, it is obvious that the intensity of the peaks in the cryogenic conditions increases when compared to as-received peak. The highest peak intensity occurred when cryogenic coolant applied from the rake face and then flank face. The increases in peak intensity and

broadening indicate hardening, which occurs on the machined surface of the workpiece [32]. Considering the hardness values given in the previous section in Fig. 6, it can be said that XRD analysis is supporting microhardness values. Another issue is that the as-received peak width is less than the machined peak widths. This has been attributed to the fact that the residual stress rate may be high in the small diameter and rolling produced receiver material. It is possible that the machining process affects the stress distribution and causes the peak to broad.

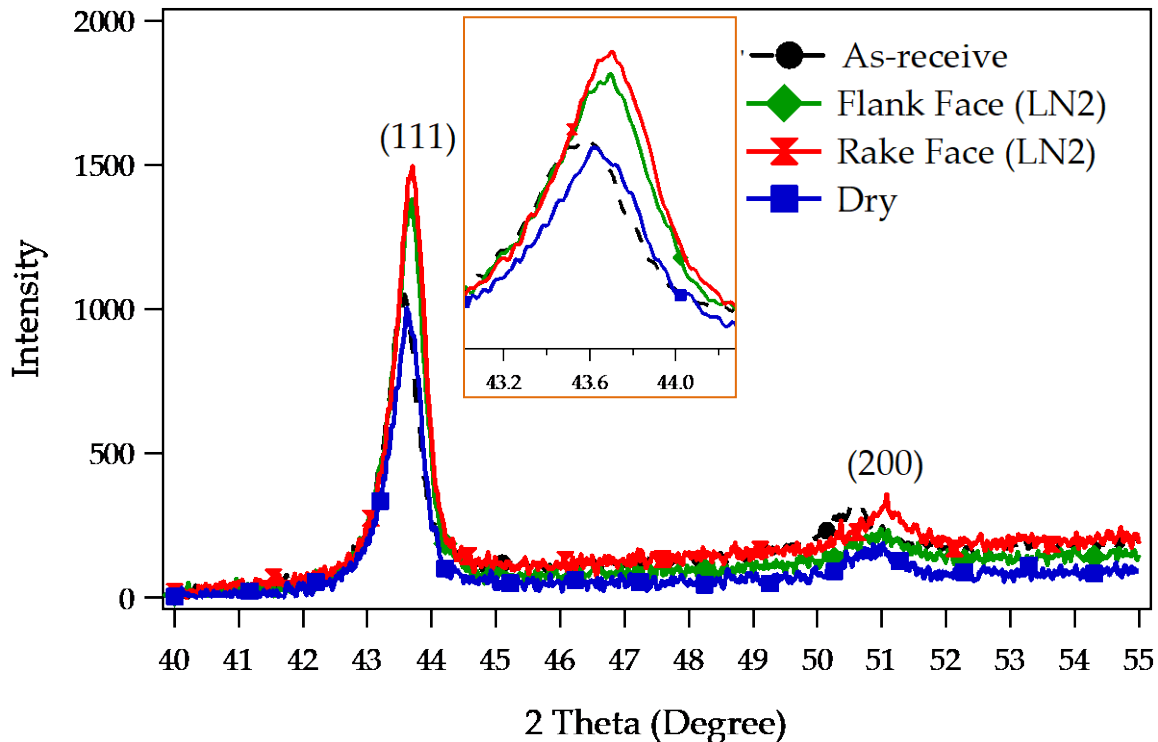


Fig. 8. XRD patterns of orthogonally machined samples under different cutting conditions ( $V=120$  m/min,  $t_o=0.16$  mm)

### Summary

In this study, machining-induced surface integrity characteristics of austenitic 316L stainless steel were examined at different cutting parameters and under cryogenic cooling conditions. Cryogenic coolant was sent to the cutting zone from different nozzle positions and its effect was examined.

- Cryogenic machining caused a decrease in cutting forces. The least cutting forces were obtained when the cryogenic coolant was applied from the rake surface.
- Apparent plastic deformation and grain refinement occurred in the microstructure of the processed material, especially under low cutting speed and cryogenic conditions.
- It is remarkable that significant hardening was observed on the machined surface and sub-surface. The highest hardness increase was obtained when cryogenic coolant was applied to the rake face.
- Cryogenically machined XRD peaks broadened more compared to dry and as-received peaks. This shows that grain refining is greater.

### Acknowledgement

Authors acknowledges the support from TUBITAK under Grant No 214M647.

### References

- [1] D. Peckner, I.M. Bernstein, Handbook of stainless steels, McGraw-Hill Book Co., New York, 1977,(Chapters paged separately), (1977).



- [2] N. Maruyama, D. Mori, S. Hiromoto, K. Kanazawa, M. Nakamura, Fatigue strength of 316L-type stainless steel in simulated body fluids, *Corrosion Science*, 53 (2011) 2222-2227. <https://doi.org/10.1016/j.corsci.2011.03.004>
- [3] M.N. Nasr, E.-G. Ng, M. Elbestawi, Modelling the effects of tool-edge radius on residual stresses when orthogonal cutting AISI 316L, *International Journal of Machine Tools and Manufacture*, 47 (2007) 401-411. <https://doi.org/10.1016/j.ijmachtools.2006.03.004>
- [4] D.A. Stephenson, J.S. Agapiou, *Metal cutting theory and practice*, CRC press, 2016.
- [5] S. Debnath, M.M. Reddy, Q.S. Yi, Environmental friendly cutting fluids and cooling techniques in machining: a review, *Journal of Cleaner Production*, 83 (2014) 33-47. <https://doi.org/10.1016/j.jclepro.2014.07.071>
- [6] E. Trent, *Metal cutting*, 1977, in, Butterworths, London.
- [7] T. Kosa, R. Ney, *Machining of stainless steels*, ASM Handbook., 16 (1989) 681-707.
- [8] V.S. Sharma, G. Singh, K. Sørby, A review on minimum quantity lubrication for machining processes, *Materials and manufacturing processes*, 30 (2015) 935-953. <https://doi.org/10.1080/10426914.2014.994759>
- [9] I. Jawahir, H. Attia, D. Biermann, J. Duflou, F. Klocke, D. Meyer, S. Newman, F. Pusavec, M. Putz, J. Rech, Cryogenic manufacturing processes, *CIRP Annals*, 65 (2016) 713-736. <https://doi.org/10.1016/j.cirp.2016.06.007>
- [10] G. Ortiz-de-Zarate, D. Soriano, A. Madariaga, A. Garay, I. Rodriguez, P. Arrazola, Experimental and FEM analysis of dry and cryogenic turning of hardened steel 100Cr6 using CBN Wiper tools, *Procedia CIRP*, 102 (2021) 7-12. <https://doi.org/10.1016/j.procir.2021.09.002>
- [11] S.Y. Hong, Y. Ding, Cooling approaches and cutting temperatures in cryogenic machining of Ti-6Al-4V, *International Journal of Machine Tools and Manufacture*, 41 (2001) 1417-1437. [https://doi.org/10.1016/S0890-6955\(01\)00026-8](https://doi.org/10.1016/S0890-6955(01)00026-8)
- [12] O. Kitay, Y. Kaynak, The effect of flood, high-pressure cooling, and CO<sub>2</sub>-assisted cryogenic machining on microhardness, microstructure, and X-ray diffraction patterns of NiTi shape memory alloy, *Journal of Materials Engineering and Performance*, 30 (2021) 5799-5810. <https://doi.org/10.1007/s11665-021-05854-6>
- [13] S.Y. Hong, Z. Zhao, Thermal aspects, material considerations and cooling strategies in cryogenic machining, *Clean Technologies and Environmental Policy*, 1 (1999) 107-116. <https://doi.org/10.1007/s100980050016>
- [14] G. Rotella, O. Dillon, D. Umbrello, L. Settineri, I. Jawahir, The effects of cooling conditions on surface integrity in machining of Ti6Al4V alloy, *The International Journal of Advanced Manufacturing Technology*, 71 (2014) 47-55. <https://doi.org/10.1007/s00170-013-5477-9>
- [15] I. Jawahir, E. Brinksmeier, R. M'saoubi, D. Aspinwall, J. Outeiro, D. Meyer, D. Umbrello, A. Jayal, Surface integrity in material removal processes: Recent advances, *CIRP Annals-Manufacturing Technology*, 60 (2011) 603-626. <https://doi.org/10.1016/j.cirp.2011.05.002>
- [16] D. Umbrello, Z. Pu, S. Caruso, J. Outeiro, A. Jayal, O. Dillon, I. Jawahir, The effects of cryogenic cooling on surface integrity in hard machining, *Procedia Engineering*, 19 (2011) 371-376. <https://doi.org/10.1016/j.proeng.2011.11.127>
- [17] S. Yang, D. Umbrello, O.W. Dillon Jr, D.A. Puleo, I. Jawahir, Cryogenic cooling effect on surface and subsurface microstructural modifications in burnishing of Co-Cr-Mo biomaterial, *Journal of Materials Processing Technology*, 217 (2015) 211-221. <https://doi.org/10.1016/j.jmatprotec.2014.11.004>
- [18] Y. Kaynak, H. Tobe, R. Noebe, H. Karaca, I. Jawahir, The effects of machining on the microstructure and transformation behavior of NiTi Alloy, *Scripta Materialia*, 74 (2014) 60-63. <https://doi.org/10.1016/j.scriptamat.2013.10.023>

- [19] S. Yang, Cryogenic burnishing of Co-Cr-Mo biomedical alloy for enhanced surface integrity and improved wear performance, in, University of Kentucky, 2012.
- [20] Y.K. Erkin Duman, Analysis of Surface Integrity in Cryogenic Machining of 316l Stainless Steel Material, in: UTIS, İstanbul, TURKEY, 2016, pp. 253-265.
- [21] M. Habak, J.L. Lebrun, An experimental study of the effect of high-pressure water jet assisted turning (HPWJAT) on the surface integrity, *International Journal of Machine Tools and Manufacture*, 51 (2011) 661-669. <https://doi.org/10.1016/j.ijmachtools.2011.05.001>
- [22] K.B. Small, D.A. Englehart, T.A. Christman, Etching specialty alloys, *Advanced materials & processes*, (2008) 33.
- [23] D. Ulutan, T. Ozel, Machining induced surface integrity in titanium and nickel alloys: A review, *International Journal of Machine Tools and Manufacture*, 51 (2011) 250-280. <https://doi.org/10.1016/j.ijmachtools.2010.11.003>
- [24] Y. Kaynak, T. Lu, I. Jawahir, Cryogenic machining-induced surface integrity: a review and comparison with dry, MQL, and flood-cooled machining, *Machining Science and Technology*, 18 (2014) 149-198.
- [25] D. O'Sullivan, M. Cotterell, Machinability of austenitic stainless steel SS303, *Journal of Materials Processing Technology*, 124 (2002) 153-159. <https://doi.org/10.1080/10910344.2014.897836> [https://doi.org/10.1016/S0924-0136\(02\)00197-8](https://doi.org/10.1016/S0924-0136(02)00197-8)
- [26] Y. Idell, G. Facco, A. Kulovits, M. Shankar, J. Wiezorek, Strengthening of austenitic stainless steel by formation of nanocrystalline  $\gamma$ -phase through severe plastic deformation during two-dimensional linear plane-strain machining, *Scripta materialia*, 68 (2013) 667-670. <https://doi.org/10.1016/j.scriptamat.2013.01.025>
- [27] R. M'Saoubi, J. Outeiro, H. Chandrasekaran, O. Dillon Jr, I. Jawahir, A review of surface integrity in machining and its impact on functional performance and life of machined products, *International Journal of Sustainable Manufacturing*, 1 (2008) 203-236. <https://doi.org/10.1504/IJSM.2008.019234>
- [28] Y. Kaynak, H. Karaca, I. Jawahir, Cutting speed dependent microstructure and transformation behavior of NiTi alloy in dry and cryogenic machining, *Journal of Materials Engineering and Performance*, 24 (2015) 452-460. <https://doi.org/10.1007/s11665-014-1247-6>
- [29] J. Patel, M. Cohen, Criterion for the action of applied stress in the martensitic transformation, *Acta Metallurgica*, 1 (1953) 531-538. [https://doi.org/10.1016/0001-6160\(53\)90083-2](https://doi.org/10.1016/0001-6160(53)90083-2)
- [30] A. Rosen, R. Jago, T. Kjer, Tensile properties of metastable stainless steels, *Journal of Materials Science*, 7 (1972) 870-876. <https://doi.org/10.1007/BF00550434>
- [31] Y. Kaynak, B. Huang, H. Karaca, I. Jawahir, Surface Characteristics of Machined NiTi Shape Memory Alloy: The Effects of Cryogenic Cooling and Preheating Conditions, *Journal of Materials Engineering and Performance*, 26 (2017) 3597-3606. <https://doi.org/10.1007/s11665-017-2791-7>
- [32] Y. Kaynak, Machining and phase transformation response of room-temperature austenitic NiTi shape memory alloy, *Journal of materials engineering and performance*, 23 (2014) 3354-3360. <https://doi.org/10.1007/s11665-014-1058-9>